

A global descriptor of spatial pattern interaction in the galaxy distribution

Martin Kerscher^{1,7}, María Jesús Pons–Bordería², Jens Schmalzing^{1,3}, Roberto Trasarti–Battistoni^{1,4}, Thomas Buchert¹, Vicent J. Martínez⁵, and Riccardo Valdarnini⁶

ABSTRACT

We present the function J as a morphological descriptor for point patterns formed by the distribution of galaxies in the Universe. This function was recently introduced in the field of spatial statistics, and is based on the nearest neighbor distribution and the void probability function. The J descriptor allows to distinguish clustered (i.e. correlated) from “regular” (i.e. anti-correlated) point distributions. We outline the theoretical foundations of the method, perform tests with a Matérn cluster process as an idealised model of galaxy clustering, and apply the descriptor to galaxies and loose groups in the Perseus–Pisces Survey. A comparison with mock-samples extracted from a mixed dark matter simulation shows that the J descriptor can be profitably used to constrain (in this case reject) viable models of cosmic structure formation.

Subject headings: methods: statistical; galaxies: clusters: general; large-scale structure of universe

1. Introduction

Three-dimensional patterns formed by the spatial distribution of galaxies in the Universe have already been described and quantified by various methods: correlation functions, counts-in-cells (Peebles 1993), the void probability function (White 1979), the genus (Melott 1990), the multi-fractal spectrum (Martínez et al. 1990), skewness and kurtosis (Gaztañaga & Frieman 1994), and

¹Ludwig–Maximilians–Universität, Theresienstraße 37, 80333 München, Germany

²Departamento de Física Teórica, Universidad Autónoma de Madrid, 28049 Cantoblanco, Madrid, Spain

³Max–Planck–Institut für Astrophysik, Karl–Schwarzschild–Straße 1, 85740 Garching, Germany

⁴Sezione di Astrofisica & Cosmologia, Dipartimento di Fisica, Univeristà di Milano, via Celoria 16, 20133 Milano, Italy

⁵Departament d’Astronomia i Astrofísica, Universitat de València, 46100 Burjassot, València, Spain

⁶SISSA, Via Beirut 2-4, 34014 Trieste, Italy

⁷email kerscher@stat.physik.uni-muenchen.de

Minkowski functionals (Mecke et al. 1994, Schmalzing & Buchert 1997). Some of these descriptors are complementary and suggest a physical interpretation of cosmic patterns by emphasising different spatial features of the galaxy distribution.

The treatment of the galaxy distribution as a realization of a spatial point process promises useful insights through the application of methods from the field of spatial statistics. The forthcoming three-dimensional galaxy catalogues with more than half a million redshifts additionally motivate the development of new statistical techniques.

In this article we want to reinforce a morphological measure for the study of the distribution of galaxies, the $J(r)$ -function, which has recently been introduced into the field of spatial statistics by van Lieshout & Baddeley (1996) and is related to the nearest-neighbor distribution $G(r)$ and the spherical contact distribution $F(r)$. Indeed, the $J(r)$ -function is equal to the first conditional correlation function (Stratonovich 1963, White 1979), and was used by Sharp (1981) to test a hierarchical ansatz for n -point correlation functions. We will focus on different features of the $J(r)$ -function showing its discriminative power as a measure of the strength of clustering.

Our article is organised as follows: In Sect. 2 we present the distribution functions F and G and show how the J function is constructed. A Matérn cluster process is considered as a simple example of a clustering point distribution. In Sect. 3 we study the clustering properties of a galaxy sample and of galaxies in groups extracted from the Perseus-Pisces redshift survey (PPS). We compare the observed galaxy distribution with mock samples extracted from a Mixed Dark Matter (MDM) simulation in Sect. 4. We summarise and conclude in Sect. 5.

2. The J function

In the theory of spatial point processes the distribution of a point's distance to its nearest neighbor is a common tool for the analysis of point patterns (Stoyan et al. 1995). We consider the redshift space coordinates $\{\mathbf{x}_i\}_{i=1}^N \in \mathbb{R}^3$ of N galaxies inside a region $D \subseteq \mathbb{R}^3$ as a realization of the point process describing the spatial distribution of galaxies in the Universe.

The nearest neighbor distribution $G(r)$ is the distribution function of the distance r of a point of the process to the nearest other point of the process. Similarly, the spherical contact distribution $F(r)$ is the distribution function of the distance r of an arbitrary point in \mathbb{R}^3 to the nearest point of the process. $F(r)$ is equal to the volume fraction occupied by the set of all points in D which are closer than r to a point of the process. Hence, $F(r)$ coincides with the volume density of the first Minkowski functional (Mecke et al. 1994 and Kerscher et al. 1997) and is related to the void probability function $P_0(r)$ via $F(r) = 1 - P_0(r)$.

For a homogeneous Poisson process we have

$$F_{\text{P}}(r) = 1 - \exp\left(-\frac{4\pi}{3}r^3n\right) = G_{\text{P}}(r), \quad (1)$$

where n is the number density. Boundary-corrected estimators for both the nearest neighbor distribution and the spherical contact distribution used in our studies are provided by minus (reduced sample) estimators (Stoyan et al. 1995, also detailed in Kerscher et al. 1998).

In a recent paper, van Lieshout & Baddeley (1996) have suggested to use the quotient

$$J(r) = \frac{1 - G(r)}{1 - F(r)} \quad (2)$$

for characterising a point process; in that way the surroundings of a point belonging to the process and the neighborhood of a random point are compared. They consider several point process models and provide limits and exact results on $J(r)$ (see also Section 2.1).

If the process under consideration is clustered, an arbitrary point usually lies farther away from a point of the process than in the case of a Poisson process. Hence, clustering is indicated by $F(r) < F_P(r)$. Consistently, $G(r) > G_P(r)$, since clustered points tend to lie closer to their nearest neighbors than randomly distributed points. So, for a clustered point distribution, $J(r) < 1$.

In case of anti-correlated, “regular” structures the situation is the opposite: on average a point of a regular process is farther away from the nearest other point of the process, so $G(r) < G_P(r)$, and a random point is closer to a point of the process, resulting in $F(r) > F_P(r)$. Therefore, regular structures are indicated by $J(r) > 1$.

For a homogeneous Poisson process we obtain $J_P(r) = 1$, separating regular from clustering structures.

2.1. The Matérn cluster process

Before attempting to apply $J(r)$ to galaxy samples, we want to test it on a model with non-trivial yet analytically tractable behaviour of $J(r)$.

In order to describe the clustering of galaxies, Neyman & Scott (1958) suggested a class of

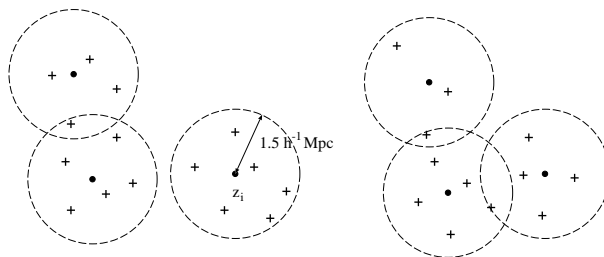


Fig. 1.— Sketch of a two-dimensional Matérn cluster process with cluster radius $R = 1.5h^{-1}\text{Mpc}$ and mean number of clusters $\mu = 5$.

point processes that was subsequently named after them. We concentrate on a subclass called Matérn cluster processes. They are constructed by first distributing uniformly M cluster centres. Around each cluster centre, which is itself not included in the final point distribution, m galaxies are placed randomly within a sphere of radius R , where m is a Poisson distributed random variable with mean μ . In Figure 1 we show a sketch of such a process. Note that overlapping clusters are allowed.

For a Matérn cluster process, van Lieshout & Baddeley (1996) proved that $J(r)$ is monotonically decreasing from 1 at $r = 0$ and attains a constant value for $r > 2R$, where R is the radius of a cluster. This constant value can be interpreted as a relic of the uniform distribution of the cluster centres. In three dimensions

$$J_M(r) = \begin{cases} \frac{1}{\text{Vol}(B_R)} \int_{B_R} e^{-\mu V(\mathbf{x}, r, R)} d^3x & \text{for } 0 \leq r \leq 2R, \\ \exp(-\mu) & \text{for } r > 2R, \end{cases} \quad (3)$$

where

$$V(\mathbf{x}, r, R) = \frac{\text{Vol}(B_r(\mathbf{x}) \cap B_R)}{\text{Vol}(B_R)} \quad (4)$$

denotes the ratio of the volume of the intersection of two balls to the volume of a single ball. Here $B_r(\mathbf{x})$ is a ball of radius r centred at the point \mathbf{x} , while B_R is a ball of radius R centred at the origin. This quantity can be calculated from basic geometric considerations, both in two (Stoyan & Stoyan 1994) and in three dimensions, where the result is

$$V(x, r, R) = \begin{cases} c_3 x^3 + c_1 x + c_0 + c_{-1} x^{-1} & \text{for } 0 \leq r < R \text{ and } R - r < x < R, \\ & \text{or } R \leq r \leq 2R \text{ and } r - R < x < r, \\ r^3/R^3 & \text{for } 0 \leq r < R \text{ and } 0 \leq x \leq R - r, \\ 1 & \text{for } R \leq r \leq 2R \text{ and } 0 \leq x \leq r - R. \end{cases} \quad (5)$$

with $x = |\mathbf{x}|$ and

$$c_3 = \frac{1}{16R^3}, \quad c_1 = -\frac{3}{8}\left(\frac{r^2}{R^3} + \frac{1}{R}\right), \quad c_0 = \frac{1}{2}\left(\frac{r^3}{R^3} + 1\right), \quad c_{-1} = \frac{3}{16}\left(\frac{2r^2}{R} - \frac{r^4}{R^3} - R\right), \quad (6)$$

In Figure 2 we show⁸ $J_M(r)$ for $R = 1.5h^{-1}\text{Mpc}$ and several values of μ ; this represents typical situations of galaxy clustering. Obviously $J(r)$ discriminates between the varying richness classes of the Matérn cluster processes.

3. Galaxy samples

In this section we want to go one step further by applying $J(r)$ to catalogues of galaxies and groups of galaxies, and compare them with a Matérn cluster process.

⁸Throughout this article, distances are given in $h^{-1}\text{Mpc}$, where h denotes the value of the Hubble parameter measured in units of $100 \frac{\text{km/s}}{\text{Mpc}}$.

3.1. Description of the PPS galaxy and group samples

The PPS database was compiled in the last decade (Giovanelli & Haynes 1991, Wegner et al. 1993). The full redshift survey is magnitude–limited down to a Zwicky magnitude of $m_Z \leq 15.7$ (Zwicky et al. 1968), and at least 95% complete to $m_Z \leq 15.5$ (see Figure 1 in Iovino et al. 1993). We extract a volume–limited subsample with $M_Z \leq -19$ and radius $79h^{-1}\text{Mpc}$, confined to $-1^h.50 \leq \alpha \leq +3^h.00$ and $0^\circ \leq \delta \leq 40^\circ$, i.e. a solid angle of 0.76sr. Redshifts are corrected for the motion of the Sun relative to the rest frame of the Cosmic Microwave Background (CMB) as in Peebles (1993), and we also correct Zwicky magnitudes for interstellar extinction as in Burstein & Heiles (1978). The final volume–limited sample PPS79 contains 817 galaxies.

To find groups, we use the redshift space friends–of–friends algorithm of Huchra & Geller (1982), suitably adapted to our case. It is a truncated percolation algorithm with two independent linking parameters D and V . Briefly, two galaxies are “friends” if their transverse and radial separations r_{ij}^\perp and r_{ij}^\parallel satisfy $r_{ij}^\perp \leq D$ and $r_{ij}^\parallel \leq V/H_0$, respectively. Friendship is transitive, and a set of *three* or more friends is called a loose group of galaxies.

Usually, loose groups are identified in magnitude–limited samples. Here, we consider only volume–limited samples. Values of $D = 0.52h^{-1}\text{Mpc}$ and $V = 600 \text{ km/s}$ give very good agreement of global properties (e.g. the total fraction of galaxies in groups, the ratio of groups to galaxies, or the median velocity dispersion) between our volume–limited group catalogue and the magnitude–limited catalogue constructed by Trasarti-Battistoni (1998).

The final sample contains 230 galaxies in 48 loose groups. A typical group has 5 observed members, a “virial mass” of some $10^{13}M_\odot$, and an observed luminosity of some $10^{10}L_\odot$. Both its radius and its inter–member pairwise separation are around $0.5h^{-1}\text{Mpc}$, and the line–of–sight velocity dispersion amounts to roughly 200 km/s, so the groups appear thin and elongated in redshift space.

3.2. $J(r)$ for the galaxy samples

We calculated $J(r)$ for all galaxies from the PPS79 sample; the results are shown in Figure 3. With $J(r)$ lying outside the area occupied by realizations of a Poisson process, one can clearly see that galaxies are strongly clustered – not a particularly surprising result. In Sect. 4.3, somewhat more interesting comparisons with galaxy mock–samples extracted from N –body simulations are performed.

Figure 4 displays the results for grouped galaxies. Since each group contains at least three members, the nearest neighbour of a grouped galaxy is certainly found within the largest link length used in the friends–of–friends procedure. Hence we observe $G(r) = 1$ and subsequently $J(r) = 0$ for $r > 5.6h^{-1}\text{Mpc}$ in the grouped galaxy sample. $J(r)$ is in general *not* invariant under changes of the number density (van Lieshout & Baddeley 1996). To compare the $J(r)$ for grouped galaxies with

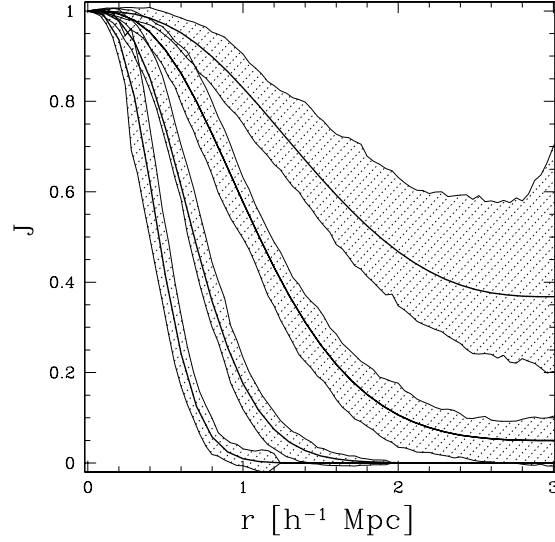


Fig. 2.— In this panel we show J_M for Matérn cluster processes with fixed cluster radius $R = 1.5h^{-1}\text{Mpc}$ and varying mean number of galaxies per cluster $\mu = 1, 3, 10, 30$ (bending down successively). The areas indicate $1\text{-}\sigma$ fluctuations of 50 realizations.

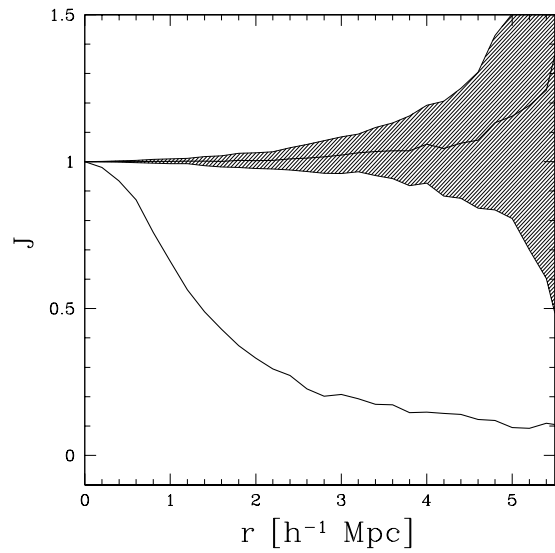


Fig. 3.— $J(r)$ for all galaxies in the PPS79 sample (solid line) and for 50 realizations of a Poisson process with the same number of points (dashed area). The dashed area indicates $1\text{-}\sigma$ fluctuations.

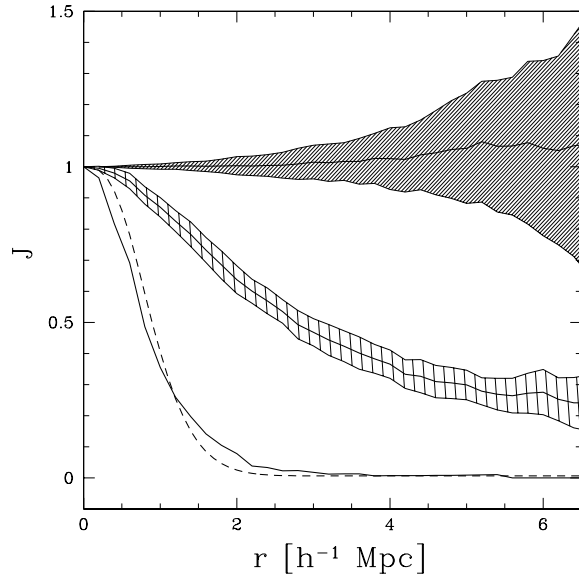


Fig. 4.— $J(r)$ for the galaxies in groups in the PPS79 sample (solid line), for a Matérn cluster process with $\mu = 5$ and $R = 1.5h^{-1}\text{Mpc}$ (dashed line), for the average of 50 samples extracted from all galaxies with the same number density as the galaxies in groups (light shaded area), and for the average and fluctuations of 50 realizations of a Poisson process (dark shaded area).

the $J(r)$ for all galaxies, we subsample the denser PPS79. $J(r)$ is calculated from 50 subsamples of 230 galaxies randomly selected from the whole PPS79 sample. With $J(r)$ we measure the strength of clustering, which is emphasised when we consider galaxies in groups only, and is less pronounced when we look at the whole sample with field galaxies included. Similarly the value of $J(r)$ for the sub-sampled PPS79 is higher than $J(r)$ for the whole PPS79, because Random sub-sampling (thinning) tends to increase $J(r)$ towards the Poisson value.

The centers of loose groups show a strong correlation themselves (Trasarti-Battistoni et al. 1997), therefore a Matérn cluster process can only serve as a rough approximation to the true distribution of galaxies in groups. Despite this, a Matérn cluster process with $\mu = 5$ galaxies per group (cluster) and a group radius of $R = 1.5h^{-1}\text{Mpc}$ shows a $J(r)$ comparable to the $J(r)$ obtained from the galaxies in groups, where in the mean 4.8 galaxies reside in a group (see Fig. 2). We see a low, almost constant value of $J(r)$ for $r > 2.5h^{-1}\text{Mpc}$. This suggests that we are indeed looking at highly clustered galaxies with small contamination by “field” galaxies.

The $J_M(r)$ of a Matérn cluster process gets constant for radii twice as large as the cluster radius. Already, van Lieshout & Baddeley (1996) express their hope to deduce a cluster scale R in a point distribution from $J(2R) \approx \text{const.}$ However, this must be taken with extreme caution. As can be seen from Fig. 2 we may be fooled by a factor of three by the fluctuations in the estimated $J(r)$. The uncertainty becomes even worse when we consider certain Cox-processes, where $J(r)$ decreases strictly monotonically towards a constant value (van Lieshout & Baddeley 1996), and in principle no scale can be deduced from the comparison with the oversimplified Matérn cluster process. Either we have to restrict ourselves to qualitative statements, or come up with more refined and realistic models.

4. Comparison with N-body simulations

The preceding section showed that the qualitative features of the galaxy distribution are well described by the J -function. In this section we explicate that the J -function is also suitable for a quantitative comparison, and allows us to constrain cosmological models.

4.1. N-body simulations and mock-catalogues

We extract 64 mock-PPS catalogues from a cosmological N-body simulation of a Mixed Dark Matter (MDM) model.

We consider a MDM model with one species of massive neutrinos, dimensionless Hubble parameter $h = 0.5$ and density parameters $\Omega_c = 0.8$, $\Omega_h = 0.2$ for cold and hot dark matter, respectively. The analytical expressions for the MDM power spectra $P(k)$ was taken from Ma (1996). The initial $P(k)$ was normalised to the COBE 4-yr data (Bunn & White 1997), giving a corresponding value

of $\sigma_8 = 0.82$ for the r.m.s. mass fluctuation in an $8h^{-1}\text{Mpc}$ sphere.

The simulation was run from an initial expansion factor $a_i = 1$ down to $a_f = 4.5$ using a P³M code with 100^3 particles of mass $1.49 \cdot 10^{13} M_\odot$, on a cubic grid of 256^3 cells, with a force softening radius $0.32h^{-1}\text{Mpc}$, in a box of side $300h^{-1}\text{Mpc}$. The integration was performed in comoving coordinates using $a(t)$ as time variable for a total of 225 steps.

We identify “galaxies” in our simulation with a method similar to the one discussed by Little & Weinberg (1994):

First, we associate with each particle a number n_i of galaxy-scale peaks calculated from the initial density contrast field $\delta(\mathbf{x})$. In the peak-background split approximation (Bardeen et al. 1986, White et al. 1987, Park 1991) n_i is the number of galaxy peaks with height $\delta_s(\mathbf{x}_i) \geq \nu_{th}\sigma_s$, where $\delta_s(\mathbf{x})$ denotes the field smoothed with a Gaussian kernel of width $R_s = 0.55h^{-1}\text{Mpc}$, and σ_s^2 gives the smoothed field’s variance. The field is subject to the constraint that it takes the value $\nu_b\sigma_b$ when smoothed on a scale $R_b > R_s$ (see Park 1991 for more details). Choosing $\nu_{th} = 0.05$, at $a = 4.5$ the particle two-point correlation function, weighted according to n_i , matches in slope and amplitude the galaxy two-point correlation function. For the adopted parameters, the total number of peaks in the box is $\sum n_i \simeq 690,000$.

Then, we select the i -th particle as a galaxy if $An_i > p$, where $p \in (0,1)$ is a uniformly distributed random variable, and A is a constant of proportionality. The latter is set by the requirement that the mean number density of “galaxies” in the box matches the mean density of $M \leq -19 + 5 \log(h)$ galaxies expected from the Schechter luminosity function with $\alpha = -1.15$, $M_* = -19.3 + 5 \log(h)$, $\phi_* = 0.02 h^3 \text{Mpc}^{-3}$ appropriate for PPS (Trasarti-Battistoni 1998; Marzke et al. 1994). This Monte-Carlo procedure makes the implicit assumption that the higher the peak, the more luminous the associated galaxy.

The mock-PPS catalogues were built as follows. The simulation cube was divided into 64 sub-cubes of side length $75h^{-1}\text{Mpc}$. Within each sub-cube we fit a PPS-like wedge of radius $79h^{-1}\text{Mpc}$. Redshift-space coordinates α, δ, cz were assigned to all the “galaxies” of the sub-cubes. Finally, we kept only the “galaxies” within the redshift-space-boundaries of the mock-PPS catalogues.

Although we are looking at a large volume with a depth $79h^{-1}\text{Mpc}$ and a solid angle of 0.76sr , we observe large fluctuations of 25% in the number of points per mock-sample (Fig. 5). This is consistent with the large-scale fluctuations of the clustering properties of IRAS galaxies, as found by Kerscher et al. (1998) out to scales of $200h^{-1}\text{Mpc}$, and expresses cosmic variance in agreement with expected sample-to-sample variations (Buchert & Martínez 1993). As we will see, this slightly complicates the analysis.

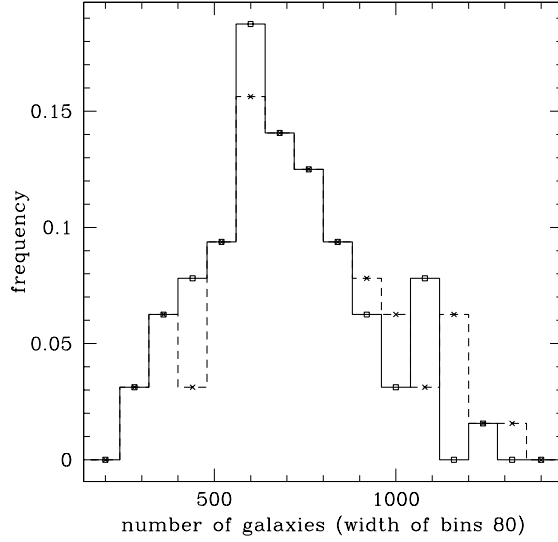


Fig. 5.— This histogram displays the number of points per mock-sample; the solid lines give the values in redshift-space, while the dashed lines corresponds to selection in real-space.

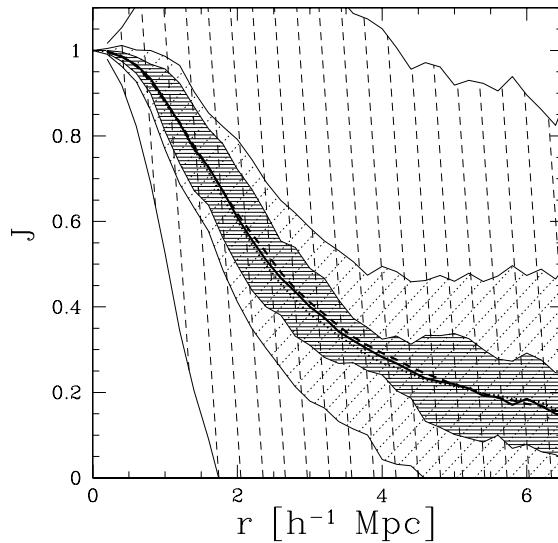


Fig. 6.— The mean $J(r)$ and the 1σ range for the mock-samples with $\Delta = 30$ (solid line, dark shaded), with $\Delta = 100$ (dotted line, medium shaded), and for all mock-samples (dashed line, light shaded, the 1σ range is plotted symmetrically).

4.2. $J(r)$ for the mock-samples

At first we investigate the mock-samples selected in redshift-space. If we use all the 64 mock-samples we are dominated by the fluctuations between samples with a different number density (see Fig. 6). Therefore, we restrict ourselves to mock-samples with approximately the same number of points as in the observed galaxy sample: $N_{\text{gal}} - \Delta \leq N_{\text{mock}} \leq N_{\text{gal}} + \Delta$, with $N_{\text{gal}} = 817$. For $\Delta = 30$ only six samples enter, whereas for $\Delta = 100$ we already have seventeen mock-samples to analyse. The mean value of $J(r)$ hardly changes between samples with different Δ . Obviously, samples with low density tend to be centred on voids, and high-density samples typically include large, Coma-like clusters. So large fluctuations in the number density lead to large fluctuations in the clustering properties measured by $J(r)$ but cancel in the mean. These fluctuations decrease for smaller Δ (see Fig. 6; this was confirmed by inspecting samples with $\Delta = 50$ and $\Delta = 200$). In order to look at structures comparable to the PPS sample we consider mock-samples with a similar number density as in the observed galaxy sample, and do not subsample the mock-samples with high number density.

In Fig. 7 the results of the mock-samples in real- and redshift-space are compared. The mock-samples selected in redshift-space show a weaker clustering than mock-samples selected in real-space on small scales out to at least $2h^{-1}\text{Mpc}$, as can be deduced from the higher $J(r)$. This can be traced back to redshift space distortions. The peculiar motions act by erasing small scale clustering; therefore the J value of redshift-space samples is larger (less clustering) than that of real-space samples. This effect changes at a given distance ($2h^{-1}\text{Mpc}$). The same effect was found by Martínez et al. (1993) in volume-limited subsamples, extracted from CfA-I, by means of the two-point correlation function.

4.3. Comparison of the PPS galaxies with the mock-samples

In Fig. 8 the results of the mock-samples in redshift-space are compared with the results of the observed galaxy distribution in the PPS. The mock-samples show insufficient clustering on small scales out to at least $3h^{-1}\text{Mpc}$, as can be deduced from the higher $J(r)$. This is probably due to the high velocity dispersion in MDM models (Jing et al. 1994). In real-space, which is *not* directly comparable with the PPS data, the mock-samples reproduce the clustering on small scales out to $1h^{-1}\text{Mpc}$, but again show not enough clustering, even though they become marginally consistent with the observed galaxy distribution on larger scales. We have to conclude that this MDM simulation is unable to reproduce the observed strong clustering of galaxies on small scales. Of course this result depends on our method of galaxy identification. A different biasing prescription might change this. On large scales a definitive answer is not possible, since for r larger than $6h^{-1}\text{Mpc}$ an estimation of $J(r)$ becomes unreliable; the empirical $G(r)$ and $F(r)$ approach unity, and the quotient $J(r)$ is ill-defined.

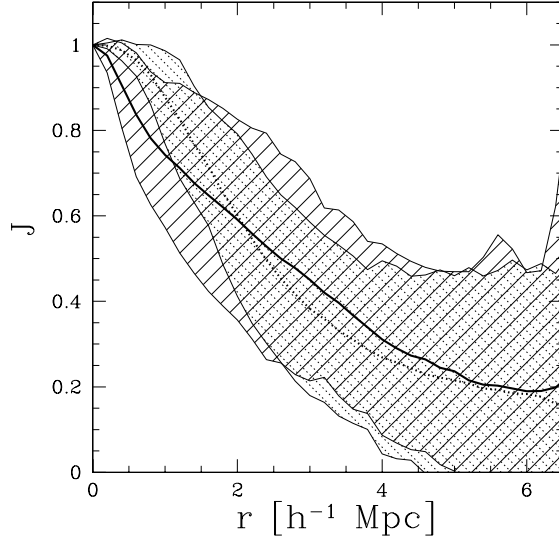


Fig. 7.— This plot shows the average value of $J(r)$ and 1σ range for the mock-samples with $\Delta = 100$ in real-space (solid lines), and for the mock-samples in redshift-space (dotted lines).

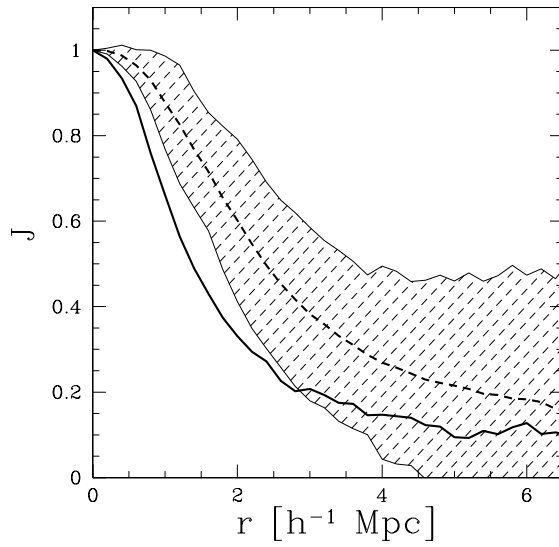


Fig. 8.— $J(r)$ is shown for the PPS79 galaxy sample (solid line) and the 1σ range for the mock-samples with $\Delta = 100$ in redshift-space (dashed area).

5. Conclusion and Outlook

We have highlighted promising properties of the global morphological descriptor $J(r)$. It connects the distribution functions $F(r)$ and $G(r)$ and, hence, incorporates all orders of correlation functions. $J(r)$ measures the strength of clustering in a point process and distinguishes between correlated and anti-correlated patterns. The example of a Matérn cluster process illustrates that $J(r)$ sensitively depends on the richness of the clusters or groups.

Since $J(r)$ is built from cumulated distribution functions, we do not encounter spurious results due to binning. This becomes particularly important on small scales.

The application of the J -function to galaxies in a volume limited sample and to a sample of galaxies in loose groups clearly showed the stronger clustering of galaxies in groups. In a comparison with a Matérn cluster we found that internal properties, like the richness of loose groups, are satisfactorily modelled. However, for the large-scale distribution of galaxies, the Matérn cluster process clearly is an over-simplification.

We used the J -function for a comparison of the observed galaxy distribution with galaxy mock-samples. Although the mock-samples extracted from a MDM-simulation cover a large volume, we detected large fluctuations of the order of 25% in the number of points per sample. On small scales, out to $1h^{-1}\text{Mpc}$, the clustering in real-space is as strong as in the observed galaxy distribution, but the comparable redshift-space mock-samples show too weak clustering. On larger scales from $2-6h^{-1}\text{Mpc}$ both real- and redshift-space mock-samples show too weak clustering. Hence, this MDM simulation is not able to reproduce the observed strong clustering of the galaxies on small scales.

The function $J(r)$ has proved to achieve comparable discriminative power as the Minkowski functionals (Kerscher et al. 1998), and is most suitable for addressing the question of “regularity” on large-scales as demonstrated in an analysis of the distribution of superclusters (Kerscher 1998). In this article we have shown that the $J(r)$ function is a useful tool for quantifying the clustering of galaxies on small scales and is capable of constraining cosmological models of structure formation.

Acknowledgements

It is a pleasure to thank Adrian Baddeley, Bryan Scott, Claus Beisbart and Herbert Wagner for useful discussions and comments. We thank Simon D.M. White for pointing out the relation to the conditional correlation function. This work was partially supported by the EC network of the program Human Capital and Mobility No. CHRX-CT93-0129, the Acción Integrada Hispano-Alemana HA-188A (MEC), the Sonderforschungsbereich SFB 375 für Astroteilchenphysik der Deutschen Forschungsgemeinschaft, and the Spanish DGES (project number PB96-0797).

REFERENCES

- Bardeen, J. M., Bond, J. R., Kaiser, N., & Szalay, A. S., ApJ **304** (1986), 15
- Buchert, T. & Martínez, V. J., ApJ **411** (1993), 485
- Bunn, E. F. & White, M., ApJ **480** (1997), 6
- Burstein, D. & Heiles, C., ApJ **225** (1978), 40
- Gaztañaga, E. & Frieman, J. A., ApJ **437** (1994), L13
- Giovanelli, R. & Haynes, M. P., ARA&A **29** (1991), 499
- Huchra, J. & Geller, M., ApJ **257** (1982), 423
- Iovino, A., Giovanelli, R., Haynes, M. P., Chincarini, G., & Guzzo, L., MNRAS **265** (1993), 21
- Jing, Y., Mo, H., Börner, G., & Fang, L. Z., Astron. Astrophys. **284** (1994), 703
- Kerscher, M., Schmalzing, J., Retzlaff, J., Borgani, S., Buchert, T., Gottlöber, S., Müller, V., Plionis, M., & Wagner, H., MNRAS **284** (1997), 73
- Kerscher, M., Schmalzing, J., Buchert, T., & Wagner, H., Astron. Astrophys. **333** (1998), 1
- Kerscher, M., Astron. Astrophys. **336** (1998), 29
- Little, B. & Weinberg, D., MNRAS **267** (1994), 605
- Ma, C.-P., ApJ **471** (1996), 13
- Martínez, V. J., Jones, B. J. T., Dominguez-Tenreiro, R., & van de Weygaert, R., ApJ **357** (1990), 50
- Martínez, V. J., Portilla, M., Jones, B. J. T., & Paredes, S., Astron. Astrophys. **280** (1993), 5
- Marzke, R., Huchra, J., & Geller, M., ApJ **428** (1994), 43
- Mecke, K. R., Buchert, T., & Wagner, H., Astron. Astrophys. **288** (1994), 697
- Melott, A. L., Physics Rep. **193** (1990), 1
- Neyman, J. & Scott, E. L., J. R. Stat. Soc. **20** (1958), 1
- Park, C., MNRAS **251** (1991), 167
- Peebles, P. J. E., *Principles of physical cosmology*, Princeton University Press, Princeton, New Jersey, 1993
- Schmalzing, J. & Buchert, T., ApJ **482** (1997), L1
- Sharp, N., MNRAS **195** (1981), 857
- Stoyan, D. & Stoyan, H., *Fractals, Random Shapes and Point Fields*, John Wiley & Sons, Chichester, 1994
- Stoyan, D., Kendall, W. S., & Mecke, J., *Stochastic Geometry and its Applications*, 2nd ed., John Wiley & Sons, Chichester, 1995
- Stratonovich, R. L., *Topics in the theory of random noise*, Vol. 1, Gordon and Breach, New York, 1963
- Trasarti-Battistoni, R., Invernizzi, G., & Bonometto, S. A., ApJ **475** (1997), 1
- Trasarti-Battistoni, R., Astron. Astrophys. Suppl. **130** (1998), 341
- van Lieshout, M. N. M. & Baddeley, A. J., Statist. Neerlandica **50** (1996), 344
- Wegner, G., Haynes, M. P., & Giovanelli, R., AJ **105** (1993), 1251
- White, S. D. M., Frenk, C. S., Davis, M., & Efstathiou, G., ApJ **313** (1987), 505
- White, S. D. M., MNRAS **186** (1979), 145
- Zwicky, F., Herzog, E., Wild, P., Karpowicz, M., & Kowal, C., *Catalogue of Galaxies and Clusters of Galaxies*, Vol. 1–6, California Inst. of Technology, Pasadena, 1961–1968